

Fe-Mediated ARGET Atom Transfer Radical Polymerization of Methyl Methacrylate in Ionic Liquid-Based Microemulsion

Guo-Xiang Wang,¹ Mang Lu,² Li-Chao Liu,¹ Hu Wu,¹ Ming Zhong¹

¹College of Chemistry and Chemical Engineering, Hunan Institute of Science and Technology, Yueyang 414006, Hunan Province, People's Republic of China

²School of Materials Science and Engineering, Jingdezhen Ceramic Institute, Jingdezhen 333403, Jiangxi Province, People's Republic of China

Correspondence to: G.-X. Wang (E-mail: wanggxwzl@163.com)

ABSTRACT: Poly(methyl methacrylate) (PMMA) was synthesized by activator regenerated by electron transfer (ARGET) atom transfer radical polymerization (ATRP) of MMA in ionic liquid-based microemulsion with polyoxyethylene sorbitan monooleate (Tween 80) as surfactant. The polymerization was carried out at 25°C with CCl₄ as initiator, FeCl₃·6H₂O/N,N,N',N'-tetramethyl-1,2-ethanediamine (TMEDA) as catalyst complex in the presence of reducing agent ascorbic acid (VC). The polymerization kinetics showed the feature of controlled/"living" process as evidenced by a linear first-order plot. The well-controlled polymers were obtained with narrow polydispersity indices and the ionic liquid-based microemulsions were transparent with a particle size less than 30 nm. The obtained polymer was characterized by ¹H NMR and gel permeation chromatography. The chain extension was successfully achieved by the obtained PMMA macroinitiator/FeCl₃·6H₂O/TMEDA/VC initiator system based on ARGET ATRP method. © 2012 Wiley Periodicals, Inc. *J. Appl. Polym. Sci.* 000: 000–000, 2012

KEYWORDS: radical polymerization; kinetics; emulsion polymerization

Received 8 May 2012; accepted 25 August 2012; published online

DOI: 10.1002/app.38517

INTRODUCTION

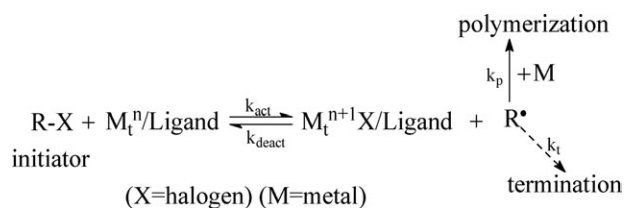
In recent years, controlled/living free radical polymerization (CLRP) has become attractive for synthesizing well-defined polymers with predetermined molecular weights and narrow polydispersity indices (PDI). Three CLRP approaches are presently studied extensively, including stable free radical polymerization (SFRP),¹ best exemplified by nitroxide-mediated polymerization (NMP), atom transfer radical polymerization (ATRP),^{2,3} and reverse addition fragmentation chain transfer polymerization.⁴ Among these techniques, ATRP is one of CLRP techniques attracting commercial interest because it is the most powerful, versatile, simple and inexpensive living polymerization. In ATRP, an equilibrium mediated by transition metal complex is established between the active growing radicals and dormant polymer chains terminated alkyl halide (Scheme 1).

However, conventional ATRP was sensitive to air and moisture due to low-oxidation transition metal complex employed in the polymerization. The limitations have been alleviated by some improved ATRP techniques, including reverse ATRP,⁵ activator generated by electron transfer (ARGET ATRP),⁶ initiator for

continuous activator regeneration (ICAR ATRP),⁷ activator regenerated by electron transfer (ARGET ATRP).⁸ These processes were carried out with high oxidation transition metal complexes tolerate air and moisture during the operation. One advantage of ARGET ATRP over ICAR ATRP is that the reducing agent does not generate new chains.

The discovery of ARGET ATRP has been recognized as a milestone contribution to the field of polymer in ATRP. In typical ARGET ATRP system, the high oxidation state metal complex can be reduced *in situ* to the low-oxidation state metal complex in the presence of the large excess of reducing agent (Scheme 2).⁹ The process is slow and the repetition reduction cycle enables the amount of catalyst to be reduced to a very low level. This is obviously beneficial to the environment.

ATRP can be carried out in different mediums such as solution, emulsion, miniemulsion and microemulsion. Microemulsion is a thermodynamically stable and optically medium formed without the requirement of external shear forces. The direct ATRP of methyl methacrylate (MMA) in microemulsion was attempted by Matyjaszewski group using a polyoxyethelence



Scheme 1. Mechanism of transition metal complex-mediated ATRP.

[(Brij98) (TM)] as surfactant and bis (2-pyridylmethyl) octadecylamine,⁹ but failed to achieve satisfactory control. In another study, AGET ATRP of n-butyl acrylate was successfully adapted in an *ab initio* emulsion polymerization with narrow PDI (1.2–1.4).¹⁰ However, the major limitation was that the relatively high concentration of catalyst was needed in polymerization.

Ionic liquids are considered as “green” solvents due to their low vapor pressures, chemical and thermal stability, non-flammability.^{11,12} In addition, ionic liquids have generally been touted as potential replacements for volatile organic solvents in many applications. There have also been some studies reporting ionic liquids behaving as selective solvents for ATRP and the easy separation of the catalyst from the products. The first report on ionic liquid as ATRP medium was reported by Carmichael group.¹³ Very recently, ionic liquid-based microemulsions have attracted significant attention combining the advantages of ionic liquid and microemulsion. Ionic liquid-based microemulsion have provided significant advantages in the sample treatment,¹⁴ chiral analysis,^{15,16} the use of pseudostationary phase (PSP),^{17,18} the addition of chemical modifier,¹⁹ and the support coating.²⁰ Furthermore, ionic liquid-based microemulsions have been applied in the field of synthesis of nano-materials,²¹ biocatalysis,²² organic reactions,²³ and polymerization.^{24–26} Yan and co-workers, have recently reported AGET ATRP of MMA at 30°C in ionic liquid microemulsion with CuCl₂/N-bis(2-pyridylmethyl)octylamine (BPMOA) as catalyst, ascorbic acid (AA) as reducing agent, ethyl 2-bromoisobutyrate (EBiB) as initiator. The molar ratios of [MMA]/[EBiB]/[CuCl₂] was 100 : 1 : 1.²⁶ The polymers obtained in ionic liquid microemulsions showed some properties different from conventional microemulsions and ionic liquid, for example, high conductivity at both room temperature and elevated temperature.²⁷

Several transition metal complexes have been applied for ATRP, including ruthenium, iron, copper, and other transition metals. Among them, iron catalyst complexes were attractive due to abundantly available, easy to handle, inexpensive and low toxicity.^{28–30} Fe-mediated ICAR ATRP has been successfully applied in ionic liquid microemulsion.²⁴ However, Fe-mediated ARGET ATRP has not been studied yet.

In this study, the well-controlled polymers of MMA were synthesized by ARGET ATRP at 25°C in ionic liquid-based microemulsion with CCl₄ as initiator, FeCl₃·6H₂O as catalyst, N,N,N',N'-Tetramethyl-1,2-ethanediamine (TMEDA) as ligand and ascorbic acid (VC) as reducing agent in the presence of the ionic liquid [bmim][PF₆]. Polyoxyethylene sorbitan monooleate (Tween 80) was used as surfactant.

EXPERIMENTAL

Materials

The ionic liquid [bmim][PF₆] was prepared according to a literature procedure.³¹ To a dry glass tube, 16.4 g (0.2 mol) of 1-methylimidazole and 23.14 g (0.25 mol) of 1-chlorobutane were added. The reaction continued at 70°C for 3 days, 1-butyl-3-methylimidazolium chloride was obtained. The solid was dissolved in deionized water. Then 41 mL of hexafluorophosphoric acid (0.25 mol) was added slowly. After the mixture was stirred overnight, an orange, viscous liquid, 1-butyl-3-methylimidazolium hexafluorophosphate was obtained.

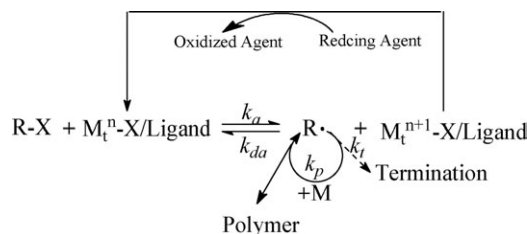
MMA was purchased from Tianjin Fuchen Chemical Reagents Factory, China and was distilled under reduced pressure before use. TMEDA and hexadecyltrimethylammonium (HTMA) were purchased from JinJinLe Industry Co., Shanghai, China. Carbon tetrachloride (CCl₄, 99%), obtained from Hunan Huihong Reagent Co., was used without further purification. 2,2'-Bipyridine (Bpy), purchased from Shanghai Yongzeng Chemical Co. China, was recrystallized twice from acetone before use. VC (AR) and Tween 80, obtained from Sinopharm Chemical Reagent Co., Shanghai, China, were used as received. Ferric chloride hexahydrate (FeCl₃·6H₂O) (AR grade) was purchased from Qingfeng Chemical Factory, Shanghai, China. Other reagents were used without further purification.

Microemulsion Region Determination

The phase diagram has been established by a conventional titration method for determination of microemulsion region. At a fixed molar ratio of mixture of [bmim][PF₆] to surfactant, MMA was gradually added under magnetic stirrer till the turbidity appeared. All mixtures were prepared by weight; and compositions are expressed as weight percent to draw the phase diagram. The experiments have been performed at 25°C and the data have been reproduced by repeating the experiments.

Polymerization

The polymerization reactions were carried out in 100-mL three necks round bottom flask equipped with a magnetic stirrer under purified nitrogen atmosphere. The mixture consisting of the surfactant Tween 80, FeCl₃·6H₂O, ionic liquid [bmim][PF₆] was stirred at room temperature to form a transparent solution. Then the organic phase containing TMEDA, MMA, and CCl₄ was added to the flask and stirred. Finally, VC was added. The amounts of components were obtained in single-phase domain according to pseudoternary phase diagram (Figure 1). The flask was placed in thermostated oil bath at 25°C. After a desired



Scheme 2. Mechanism of transition metal complex-mediated ARGET ATRP.

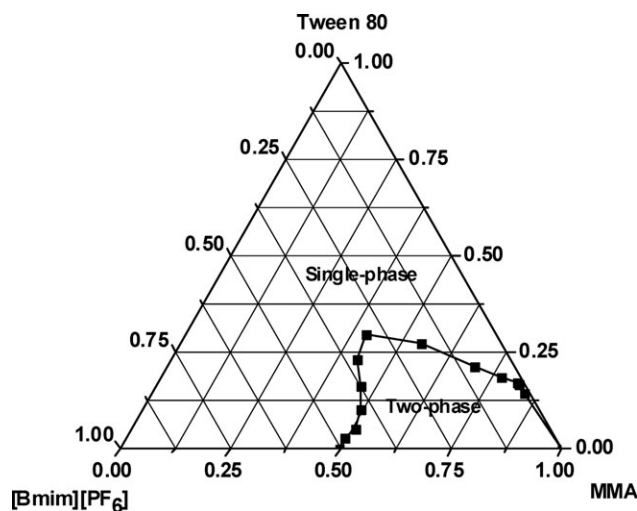


Figure 1. Pseudoternary phase diagram of a system containing surfactant (Tween 80), oil (MMA), and ionic liquid [bmim][PF₆] at 25°C.

time, the polymerization was terminated by cooling the flask into ice water. The polymer was precipitated with methanol and dried at 60°C under vacuum to a constant weight. The monomer conversions were determined gravimetrically. The compositions of each reaction are shown in Table I.

Chain Extension of Poly(methyl methacrylate) (PMMA)

The chain extension was carried out at 25°C in ionic liquid-based microemulsion. The earlier synthesized PMMA was used as macroinitiator. First, a predetermined quantity of the purified PMMA macroinitiator was added to the transparent microemulsion in three necks round bottom flask equipped with a magnetic stirrer under purified nitrogen atmosphere. Second, predetermined quantity of MMA, FeCl₃·6H₂O, and TMEDA was

added, respectively. Finally, the VC was added to initiate the polymerization reaction.

Characterization

¹H NMR spectra were recorded on a Bruker 400 MHz NMR at room temperature using CDCl₃ solvent and tetramethylsilane as internal standard. The number average molecular weight (*M_n*) and molecular weight distribution or PDI values of polymers were measured on a Waters 1515 gel permeation chromatography (GPC) system, equipped with refractive index detector, using HR1, HR3, and HR4 column with molecular weight range 100–500,000. Tetrahydrofuran was used as an eluent at a flow rate of 1.0 mL/min. The molecular weight analysis was performed at 30°C based on the universal calibration procedure with polystyrene narrow standards. Final latex particles were measured with a Zetasizer (3000 HSA, Malvern) at a fixed scattering angle of 90°. The basic principle for measuring size distribution is based on the technique of dynamic light scattering.

RESULTS AND DISCUSSION

The ternary phase diagrams of the [bmim]PF₆/Tween 80/MMA system at 25°C determined in this work by direct observation are illustrated in Figure 1. Above the phase separation boundary curve, the system exists as one phase region and the biphasic region.

The polymerization of MMA was carried out at 25°C in [bmim][PF₆]/Tween 80/MMA ionic liquid-based microemulsion system using ARGET ATRP process. The molar ratio of [MMA]₀/[CCl₄]₀/[FeCl₃·6H₂O]₀/[TMEDA]₀/[VC]₀ was fixed at 3000 : 1 : 0.1 : 0.2 : 0.5. The amount of [bmim]PF₆ was 20 mmol. The weight ratio of MMA and Tween 80 was 22.9% (wt).

Figure 2 shows kinetic plot of ln([M]₀/[M]) versus reaction time. Linear ln([M]₀/[M]) versus reaction time plot was

Table I. Compositions for Ionic Liquid Microemulsion Runs

Run	R ^a	L ^b	[bmim]PF ₆ (mmol)	[MMA] : [Tween 80] wt %	d ^c (nm)
1-Ligands	3000 : 1 : 0.1 : 0.2 : 0.5	TMEDA	20	22.9	26
	3000 : 1 : 0.1 : 0.2 : 0.5	HTMA	20	22.9	28
	3000 : 1 : 0.1 : 0.2 : 0.5	Bpy	20	22.9	28
2-Ligands	3000 : 1 : 0.1 : 0 : 0.5	TMEDA	20	22.9	26
	3000 : 1 : 0.1 : 0.1 : 0.5	TMEDA	20	22.9	25
	3000 : 1 : 0.1 : 0.2 : 0.5	TMEDA	20	22.9	27
	3000 : 1 : 0.1 : 0.5 : 0.5	TMEDA	20	22.9	29
3-MMA	2000 : 1 : 0.1 : 0.2 : 0.5	TMEDA	20	22.9	25
	3000 : 1 : 0.1 : 0.2 : 0.5	TMEDA	20	22.9	26
	4000 : 1 : 0.1 : 0.2 : 0.5	TMEDA	20	22.9	28
	5000 : 1 : 0.1 : 0.2 : 0.5	TMEDA	20	22.9	29
4-Tween 80	3000 : 1 : 0.1 : 0.2 : 0.5	TMEDA	20	16.3	29
	3000 : 1 : 0.1 : 0.2 : 0.5	TMEDA	20	33.1	24
	3000 : 1 : 0.1 : 0.2 : 0.5	TMEDA	20	63.5	16

^aR = [MMA]₀ : [CCl₄]₀ : [FeCl₃·6H₂O]₀ : [TMEDA]₀ : [VC]₀, ^bL = ligand, ^cd = average diameter.

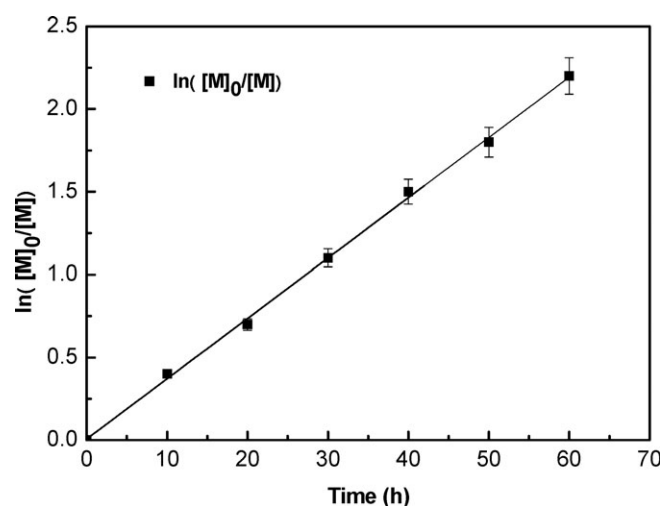


Figure 2. The kinetic plot for ARGET ATRP of MMA catalyzed by $\text{FeCl}_3 \cdot 6\text{H}_2\text{O}$ /TMEDA at 25°C in ionic liquid-based microemulsion.

observed for ARGET ATRP of MMA in ionic liquid-based microemulsion, indicating that the polymerization is approximately first-order kinetics with respect to monomer concentration. This result indicates that the concentrations of the propagating active radicals remained constant during the polymerization process and the termination can be neglected. The apparent rate constant (k_{app}) for ARGET ATRP of MMA at 25°C in ionic liquid-based microemulsion was determined from the initial slope of the semi-logarithmic kinetic plot. The calculated k_{app} value was $1 \times 10^{-5} \text{ s}^{-1}$. The reported k_{app} value for Fe-mediated ICAR ATRP of MMA carried out with in ionic liquid microemulsion was $k_{\text{app}} = 8.47 \times 10^{-5} \text{ s}^{-1}$.²⁴ This may be the different polymerization reaction temperature.

Figure 3 presents M_n and PDI for ARGET ATRP of MMA in ionic liquid-based microemulsion. As shown, the M_n increased with conversion and the experimental molecular weights ($M_{n,\text{GPC}}$) were in good agreement with the theoretical values ($M_{n,\text{th}}$) even at high conversion, ($M_{n,\text{th}}$) calculated from the following equation: $M_{n,\text{th}} = ([M]_0/[I]_0) \times W_{\text{MMA}} \times x$, where, $[M]_0$ and $[I]_0$ are the initial concentrations of the monomer and initiator, respectively; W_{MMA} is the molecular weight of the monomer and x is the monomer conversion. The PDIs decreased as the conversion increased and remained relatively low when the conversion was beyond 50% ($\text{PDI} < 1.28$). These results confirm that ARGET ATRP of MMA proceeded in a controlled manner in ionic liquid-based microemulsion.

On the basis of results discussed above, it can be concluded that ARGET ATRP of MMA in ionic liquid-based microemulsion with $[\text{FeCl}_3 \cdot 6\text{H}_2\text{O}]_0/[\text{TMEDA}]_0$ as the system is accessible.

Effect of Different Ligand on the Polymerization

The ligand plays an important role in solubilizing the transition metal salt in the media and alters the redox potential of the metal center for the appropriate dynamics of exchange between the dormant and active species with atom transfer reaction.³² The polymerization rate depends on the nature of the binding site of the ligand. The effect of ligand on the polymerization

was tested. Three different ligands were employed in these experiments. In all experiments, the molar ratio of $[\text{MMA}]_0/[\text{CCl}_4]_0/[\text{FeCl}_3 \cdot 6\text{H}_2\text{O}]_0/[\text{ligand}]_0/[\text{VC}]_0$ was kept at $3000 : 1 : 0.1 : 0.2 : 0.5$.

As can be seen from Table II, fast and controlled polymerization were observed when TMEDA were used as catalyst, with the conversion of 82.66% within 48 h. However, the conversion only reached 47.17% within 72 h and 61.28% within 50 h when the polymerization was mediated by HTMA or Bpy, respectively. Therefore, these results imply that the ARGET ATRP of MMA mediated by TMEDA possessed a higher ratio of activation/deactivation rate than that mediated by HTMA or Bpy. The key issue is ascribed to different molecular structure. HMTA used increased the steric effect of catalyst and slowed down the deactivation reaction of radical of HMTA, causing radical termination. This also indicates that the ligand played an important role in living radical polymerization. Moreover, The experimental average molecular weight ($M_{n,\text{GPC}}$) increased with monomer conversion and matched the theoretical one with narrow PDI ($1.22 < \text{PDI} < 1.27$).

Effect of Molar Ratio of $[\text{FeCl}_3 \cdot 6\text{H}_2\text{O}]_0/[\text{TMEDA}]_0$ on the Polymerization

The effect of molar ratio of $[\text{FeCl}_3 \cdot 6\text{H}_2\text{O}]_0/[\text{TMEDA}]_0$ on the polymerization was investigated. The results are shown in Table III. As seen, the polymerization rate increased with increasing concentration of ligand. The conversion reached 32.8% within 48 h when the molar ratio of $[\text{CCl}_4]_0/[\text{FeCl}_3 \cdot 6\text{H}_2\text{O}]_0/[\text{TMEDA}]_0$ was $1 : 0.1 : 0$. With increasing the molar ratio of $[\text{CCl}_4]_0/[\text{FeCl}_3 \cdot 6\text{H}_2\text{O}]_0/[\text{TMEDA}]_0 = 1 : 0.1 : 0.5$, the conversion reached 54.43% within 16 h. The $M_{n,\text{GPC}}$ increased with conversion and agreed fairly well with the $M_{n,\text{th}}$ values. PDI was broader in the absence of ligand ($\text{PDI} = 1.74$). This result confirms the polymerization proceeded in a typical free radical polymerization process.

Effect of Molar Ratio of $[\text{MMA}]_0/[\text{CCl}_4]_0$ on the Polymerization

The number of polymer chains growing is dependent upon the nature of initiator. The effect of molar ratio of $[\text{MMA}]_0/[\text{CCl}_4]_0$

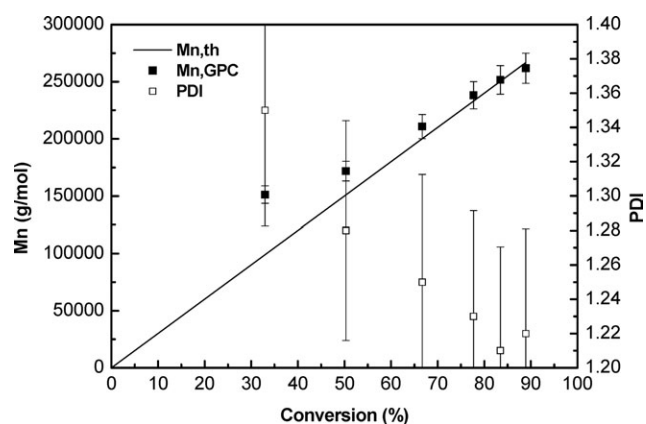


Figure 3. Dependence of number molecular weights and PDI for ARGET ATRP of MMA in ionic liquid-based microemulsion.

Table II. ARGET ATRP of MMA in Ionic Liquid Based Microemulsion With Different Ligands at 25°C

Run	Ligand	Time (h)	Conversion (%)	$M_{n,th}$ (g/mol)	$M_{n,GPC}$ (g/mol)	PDI
1	TMEDA	48	82.66	247980	251300	1.22
2	HTMA	72	47.17	141510	152700	1.27
3	Bpy	50	61.28	213840	223900	1.23

Table III. ARGET ATRP of MMA in Ionic Liquid Based Microemulsion With Different Molar Ratio of $[CCl_4]_0/[FeCl_3 \cdot 6H_2O]_0/[TMEDA]_0$ at 25°C

Run	$[CCl_4]_0/[FeCl_3 \cdot 6H_2O]_0/[TMEDA]_0$	Time (h)	Conversion (%)	$M_{n,th}$ (g/mol)	$M_{n,GPC}$ (g/mol)	PDI
1	1 : 0.1 : 0	48	32.8	98400	112800	1.74
2	1 : 0.1 : 0.1	24	46.21	138630	146700	1.28
3	1 : 0.1 : 0.2	21	53.74	161220	177200	1.26
4	1 : 0.1 : 0.5	16	54.43	163290	186400	1.31

Table IV. ARGET ATRP of MMA in Ionic Liquid Based Microemulsion With Different Molar Ratio of $[MMA]_0/[CCl_4]_0$ at 25°C

Run	$[MMA]_0/[CCl_4]_0$	Time (h)	Conversion (%)	$M_{n,th}$ (g/mol)	$M_{n,GPC}$ (g/mol)	PDI
1	2000 : 1	20	60.72	121440	132500	1.24
2	3000 : 1	24	58.81	176430	191800	1.26
3	4000 : 1	24	52.43	209720	217400	1.28
4	5000 : 1	32	45.56	227800	244700	1.35

on the polymerization was assessed. The data are demonstrated in Table IV.

As can be seen from Table IV, the polymerization rate increased with increasing the molar ratio of $[MMA]_0/[CCl_4]_0$, which can be attributed to more radical being generated by the decomposition of initiator. The $M_{n,GPC}$ values are in good agreement with the $M_{n,th}$ values and the PDI were low ($1.24 < PDI < 1.35$). However, higher concentration of initiator resulted in fast polymerization with less equilibration between chains, as evidenced by higher PDIs values with increasing the concentration of initiator.

Effect of Amount of Surfactant on Polymerization

The amount of surfactant is one of the important factors as regards the stability of an ionic liquid-based microemulsion and its subsequent polymerization. The effect of amount of surfactant on polymerization was investigated (Table V).

As shown in Table V, the polymerization conversion increased from 16.52% to 47.33% with increasing the amount of surfactant from 16.3% to 63.5% at the same time. The $M_{n,GPC}$ values

are consistent with the corresponding $M_{n,th}$ values with PDI values (1.34–1.44). The diameter decreased from 29 to 16 nm as the conversion increased. This is because larger surface areas between the continuous and dispersed phases protected by the adsorbed surfactant become possible as the surfactant concentration increases. Figure 4 presents a plot of particle size distribution for PMMA particles synthesized with different amount of surfactant in the ionic liquid-based microemulsion system. As can be seen Figure 4, the particle size distribution centered at 29 nm, 24 nm, 16 nm, respectively.

Analysis of Chain End and Chain Extension

The PMMA prepared by ARGET ATRP in ionic liquid-based microemulsion was characterized by 1H NMR (Figure 5). The chemical shift at 3.79 ppm (d in Figure 5) corresponded to the methoxy group next to the halogen chain end, and was consistent with what Sawamoto reported.³³ This result confirmed the presence of the $-Cl$ group. The chemical shift at 3.61 ppm (c in Figure 5) was assigned to the protons of methoxy group in the main chain.³³ The peak at 1.82 ppm (b in Figure 5) was attributed to the protons of methyl groups and methylene

Table V. ARGET ATRP of MMA in Ionic Liquid Based Microemulsion With Different Amount of Surfactant at 25°C

Run	$[MMA] : [Tween\ 80]$ wt %	Time (h)	Conversion (%)	$M_{n,th}$ (g/mol)	$M_{n,GPC}$ (g/mol)	PDI	d (nm)
1	16.3		16.52	49560	77400	1.34	29
2	33.1	24	27.94	83820	106600	1.36	24
3	63.5		47.33	141990	164300	1.44	16

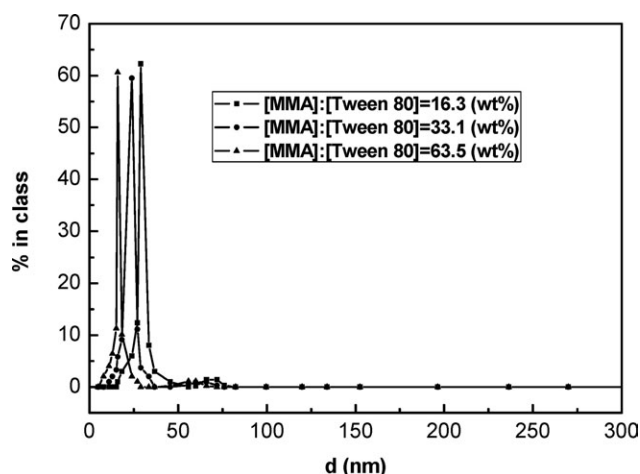


Figure 4. Particle size distribution of PMMA for the ARGET ATRP of MMA in ionic liquid-based microemulsion system.

group, respectively. The chemical shift at 0.8–1.3 ppm (a in Figure 5) was assigned to the protons of methyl groups. Thus, the obtained PMMA-Cl should be used as macroinitiator in chain extension. As shown in Figure 6, there was a peak shift from the macroinitiator PMMA-Cl ($M_{n, GPC} = 2,10,800$ g/mol, PDI=1.25) to the chained PMMA ($M_{n, GPC} = 3,82,200$ g/mol, PDI = 1.34). The living feature of the obtained PMMA-Cl was verified.

CONCLUSIONS

The results demonstrated that Fe-mediated ARGET ATRP of MMA was successfully carried out at 25°C in ionic liquid-based microemulsion with Tween 80 as surfactant. The polymerization obeyed the first-order kinetics, indicating that the polymerization proceeded in a controlled/"living" process and

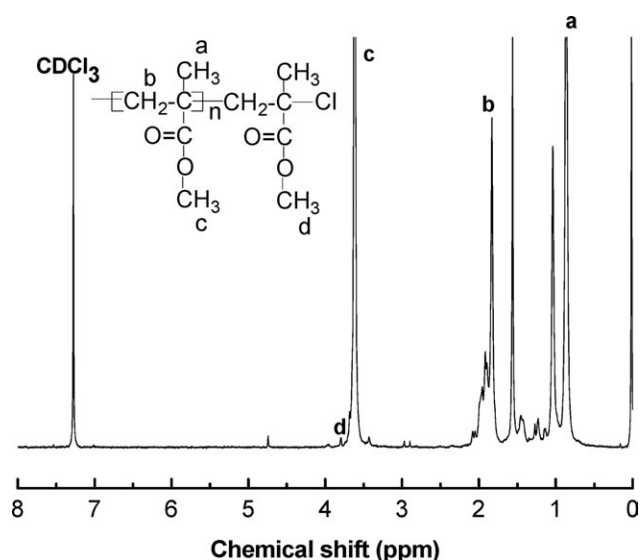


Figure 5. ^1H NMR spectrum of PMMA prepared with $[\text{MMA}]_0/[\text{CCl}_4]_0/[\text{FeCl}_3 \cdot 6\text{H}_2\text{O}]_0/[\text{TMEDA}]_0/[\text{VC}]_0$ in ionic liquid-based microemulsion.

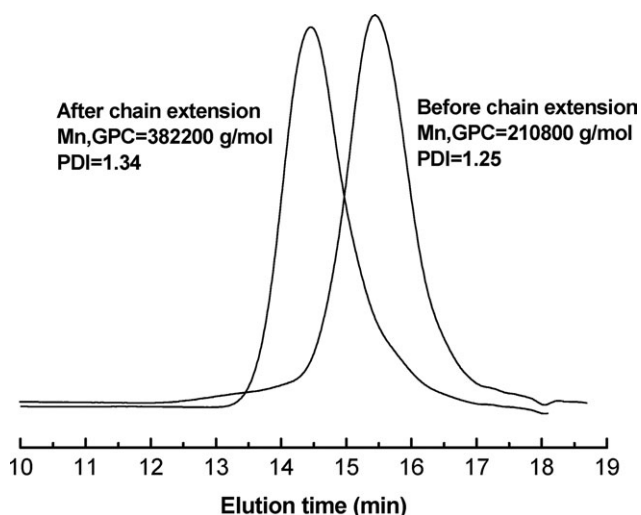


Figure 6. GPC traces before and after chain extension with PMMA as a macroinitiator.

the well-defined polymers with narrow PDI were obtained. The ionic liquid-based microemulsion was transparent throughout the polymerization process. The polymerization was controlled when the molar ratio of $[\text{CCl}_4]_0/[\text{FeCl}_3 \cdot 6\text{H}_2\text{O}]_0/[\text{TMEDA}]_0$ was 1 : 0.1 : 0.2. The polymerization rate increased with increasing the ratio of $[\text{MMA}]_0/[\text{CCl}_4]_0$ and the amount of surfactant.

REFERENCES

- Szkurhan, A. R.; Georges, M. K. *Macromolecules* **2004**, *37*, 4776.
- Xue, L.; Agarwal, U. S.; Lemstra, P. J. *Macromolecules* **2002**, *35*, 8650.
- Golas, P. L.; Louie, S.; Lowry, G. V.; Matyjaszewski, K.; Tilton, R. D. *Langmuir* **2010**, *26*, 16890.
- Lansalot, M.; Davis, T. P.; Heuts, J. P. A. *Macromolecules* **2002**, *35*, 7582.
- Li, M.; Min, K.; Matyjaszewski, K. *Macromolecules* **2004**, *37*, 2106.
- Kwiatkowski, P.; Jurczak, J.; Pietrasik, J.; Jakubowski, W.; Mueller, L.; Matyjaszewski, K. *Macromolecules* **2008**, *41*, 1067.
- Zhu, G.; Zhang, L.; Zhang, Z.; Zhu, J.; Tu, Y.; Cheng, Z.; Zhu, X. L. *Macromolecules* **2011**, *44*, 3233.
- Nicolaÿ, R.; Kwak, Y.; Matyjaszewski, K. *Angew. Chem. Int. Ed.* **2010**, *49*, 541.
- Min, K.; Matyjaszewski, K. *Macromolecules* **2005**, *38*, 8131.
- Min, K.; Gao, H. F.; Matyjaszewski, K. *J. Am. Chem. Soc.* **2006**, *128*:10521.
- Aslanov, L. A. *J. Mol. Liq.* **2011**, *162*, 101.
- Kubisa, P. *J. Polym. Sci. Part A: Polym. Chem.* **2005**, *43*, 4675.
- Carmichael, A. J.; Haddleton, D. M.; Bon, S. A. F.; Seddon, K. R. *Chem. Commun.* **2000**, 1237.

14. López Pastor, M.; Domínguez-Vidal, A.; Ayora-Cañada, M. J.; Simonet, B. M.; Lendl, B.; Valcárcel, M. *Anal. Chem.* **2008**, *80*, 2672.
15. Mwongela, S. M.; Numan, A.; Gill, N. L.; Agbaria, R. A.; Warner, I. M. *Anal. Chem.* **2003**, *75*, 6089.
16. Rizvi, S. A. A.; Shamsi, S. A. *Anal. Chem.* **2006**, *78*, 7061.
17. Borissova, M.; Palk, K.; Koel, M. *J. Chromatogr. A* **2008**, *1183*, 192.
18. Yanes, E. G.; Gratz, S. R.; Baldwin, M. J.; Robison, S. E.; Stalcup, A. M. *Anal. Chem.* **2001**, *73*, 3838.
19. Borissova, M.; Gorbats'ova, J.; Ebber, A.; Kaljurand, M.; Koel, M.; Vaher, M. *Electrophoresis* **2007**, *28*, 3600.
20. Corradini, D.; Nicoletti, I.; Bonn, G. K. *Electrophoresis* **2009**, *30*, 1869.
21. Zhao, M. W.; Zheng, L. Q.; Bai, X. T.; Li, N.; Yu, L. *Colloids Surf. A* **2009**, *346*, 229.
22. Moniruzzaman, M.; Kamiya, N.; Nakashimaa, K.; Goto, M. *Green Chem.* **2008**, *10*, 497.
23. Zhang, G. P.; Zhou, H. H.; Hu, J. Q.; Liu, M.; Kuang, Y. F.; Wang, G. X.; Lu, M.; Wu, H. *Polymer* **2012**, *53*, 1093.
24. Zhang, G. P.; Zhou, H. H.; Zhang, J. L.; Han, Xue.; Chen, J. H.; Kuang, Y. F. *J. Appl. Polym. Sci.* **2012**, *125*, 2342.
25. Zhou, Y. X.; Qiu, L. H.; Deng, Z. J.; Texter, J.; Yan, F. *Macromolecules* **2011**, *44*, 7948.
26. Yu, S. M.; Yan, F.; Zhang, X. W.; You, J. B.; Wu, P. Y.; Lu, J. M.; Xu, Q. F.; Xia, X. W.; Ma, G. L. *Macromolecules* **2008**, *41*, 3389.
27. Kanazawa, A.; Satoh, K.; Kamigaito, M. *Macromolecules* **2011**, *44*, 1927.
28. Wang, G. X.; Lu, M.; Zhong, M.; Wu, H. *J. Polym. Res.* **2012**, *19*, 9782.
29. Wang, G. X.; Wu, H. *Polym. Bull.* **2011**, *67*, 1809.
30. Huddleston, J. G.; Rogers, R. D. *Chem. Commun.* **1998**, 1765.
31. Haddleton, D. M.; Crossman, M. C.; Dana, B. H.; Duncalf, D. J.; Heming, A. M.; Kukulj, D.; Shooter, A. J. *Macromolecules* **1999**, *32*, 2110.
32. Ando, T.; Kamigaito, M.; Sawamoto, M. *Macromolecules* **1997**, *30*, 4507.